[10] Yunes, R.A.; Terenzani, A.J.; Amaral, L. do; *J.Am. Chem.Soc.* (1975) *97*, 368.
[11] Pizzolatti, M.G.; "Catálise ácida-básica e mecanismo de formação de azoxiarenos" Tese, UFSC, 1983.
[12] Bowman, D.F.; Brokenshire, J.L.; Gillan, T.; Ingold, K.U.; *J.Am.Chem.Soc.* (1971) *93*, 6551.
[13] Walters, W.A.; *J.Chem.Soc. Perkin Trans. II* (1979) 1078.
[14] Pizzolatti, M.G.; Yunes, R.A.; Trabalho enviado para publicação.
[15] Knight, G.T.; Saville, B.; *J.Chem.Soc. Perkin Trans. II* (1973) 1550.

ARTIGO

SPECTROSCOPIC PROPERTIES OF TRANSITION ELEMENTS AND THEIR RELATED MAGNETIC PROPERTIES

Pierre Porcher

Laboratoire des Eléments de Transition dans les Solides, ER210 du CNRS. 1, Place A. Briand 92195 Meudon-Bellevue, France

O.L. Malta

Departamento de Química Fundamental – UFPE, Cidade Universitária; 50739 – Recife (PE)

Recebido em 27/4/88

ABSTRACT

Optical and magnetic properties of transition elements (nd^N and nf^N ions) are re-analysed. The aim of the work is to see up to where a unique set of phenomenological parameters, those introduced in the crystal-ligand field theory described on the $|\alpha SLJM>$ basis, can describe the experimental data.

I – INTRODUCTION

The simulation of the energy level sequences of f electrons has received great attention since thirty years. After the pioner works of Racah in the forties, Stevens, Wybourne, Judd and more recently Newman and others have developed a complete set of mathematical tools, known as the Racah algebra, to describe the main forces which co-exist in a pluri-electronic system. [1]

The advantage of the rare earth ions and -less evidently- of the actinide ions is the fact that the optically active f electrons are not -or quite not- acting in the chemical bonding. They are protected by an external electron sheet. As a first consequence, only small differences exist between the energy level of the free ion and the one of the ion embedded in a cristalline matrix. Optical transitions exhibit narrow lines, characterizing transitions between electronic levels, with a small effect of vibronic couplings. On the other hand, the important degeneracy of the f^N configurations and the great number of observed levels authorize the theoretician to precisely analyse and quantify the magnitude of various interactions through phenomenological parameters. It is also possible to test ab-initio models, like for the crystal field.[2] Simulations yield rms deviations lower than 20 cm^{-1} by using about 20 phenomenological parameters, the order of magnitude of many of them is known before the simulation and some others have a second order influence.

The external d electrons of the $3d^N$ series are both "optical" and "bonding" active, with many consequences: enlargement of the optical bands due to phonon coupling, doubt about zero phonon line positions, strong effect of the ligand on both the crystal field strength and the overlap between central ion and ligand wavefunctions and, finally, a relatively poor energy level sequence. Of course, the strength of the interactions is different with a crystal field 20 times stronger, a spin-orbit coupling smaller, and also less phenomenological parameters.

From these differences, the type of simulation changes. The rare earthist takes into account up to "exotical" interactions whose order of magnitude is some wavenumber units. The d-ist uses crude approximations in order to diminue the number of interactions or, at least, the number of parameters. This is why the famous Tanabé-Sugano diagrams were so successfully employed, with Slater radial integrals F_2 and F_4 (B and C for the d-ist), fixed to hydrogenic ratio, with spin-orbit often neglected and the crystal field approximated to a cubic symmetry (D_q). The symmetry sometimes is lowered by an additional perturbation potential (D_t and D_s). Thus, the basis of the vectorial space ($|SM_sLM_L>$ for the d's and $|SLJM>$ for the f's), and even the name of the states (called from their irreducible representation for the d, from the free ion states for the f) is different.

Whatever the configuration and its description, a consequence of the diagonalisation of the secular determinant is an expression for the wavefunction associated to a given energy level. It is necessary for magnetic propertys calculations, like g values, the paramagnetic susceptibility (or effective moment) and its variation with temperature. For f electrons, the application of the magnetic tensor $L+g_eS$ on the wavefunction gives good simulation of the data. For the d electrons, on the contrary, one has to modify the operator for an a-posteriori correction of the oversimplified model for the energy level calculations (for example "anisotropic reduction of the orbital moment".[3]

II – THE INTERACTIONS

In the central field approximation the ground configuration is supposed to be well isolated from the rest of the configuration series, even if their influences are taken into account. The degeneracy of the configuration is the number of Slater determinants we can construct with all possible combinations of angular moment $m\ell$ and spin m_s quantum numbers. Its value is (N=number of electron), (table 1):

$$N!\ \frac{(2\ell+2)!}{(4\ell-2-N)!}$$

Number and type of elec.	Num. of Terms ^{2S+1}L	Num. of levels $^{2S+1}L_J$	Configuration Degeneracy
1 (5) p	1	2	8
2 (4) p	3	5	15
3 p	3	5	20
1 (9) d	1	2	10
2 (8) d	5	9	45
3 (7) d	8	19	120
4 (6) d	16	34	210
5 d	16	37	252
1 (13) f	1	2	14
2 (12) f	7	13	91
3 (11) f	17	41	364
4 (10) f	47	107	1001
5 (9) f	73	198	2002
6 (8) f	119	295	3003
7 f	119	327	3432

Table 1. Splitting of configurations ℓ^N as a function of the nature of spectroscopic operators. When the symmetry is low, the number of levels is equal to the degeneracy (respec. half) for configurations with an even (respec. odd) number of electrons.

II.1 – The free ion interactions

The first interaction corresponds to the energy separation between the ground configuration and excited ones. The corresponding parameter is E_o (or F_o).

The other main interactions are (table 2):

- the electrostatic repulsion, H_{RE}, creating the spectroscopic terms ^{2S+1}L, with (2S+1)(2L+1) as remaining degeneracy.
- the spin-orbit coupling, H_{so}, creating the spectroscopic levels $^{2S+1}L_J$, where J is the total angular momentum. The remaining degeneracy is 2J+1.

Interactions/Parameters	Nd^N	Nf^N
Electrostatic repulsion	E_0, E_1, E_2 or F_0, F_2, F_4	E_0, E_1, E_2, E_3 or F_0, F_2, F_4, F_6
Spin-orbit coupling	ξ	ξ
Configurations interac.	α, β, γ	α, β, γ
Three-body interactions	not used	$T\lambda$
Spin-spin interaction Spin-other-orbit interac.]	not used	M^k k = 0, 2, 4
Spin-other-orbit interac. (other configuration)	not used	p^k k = 2, 4, 6
Crystal field		
one electron	B_{kq} k = 2, 4	B_{kq} k = 2, 4, 6
two electrons	c^k k = 2, 4	c^k k = 2, 4, 6

Table 2. Phenomenological parameters

Less important interactions are (by their orders of magnitude):

- electrostatic interactions, H_1, between ground and excited configurations.
- three-body electrostatic interaction, H_2, for configurations having more than two equivalent electrons.
- magnetic interactions, H_3, corresponding to the spin-spin and spin-other-orbit relativistic corrections.
- two-body spin-orbit interactions, H_4, between different configurations.

II.2 – Crystal field interactions

When embedded in a crystalline matrix, the ion is submitted to an electric potential, having the same symmetry as the crystallographic ion point group. This interaction lifts more or less completely the residual degeneracy of the free ion, according to group theory rules. It creates the crystal field levels $^{2S+1}L_{JM}$ (on the $|\alpha SLJM>$ basis). Two types of crystal fields are considered (table 2):

- one-electron crystal field, H_{1cc},, with its electrostatic origin.
- two-electron crystal field, H_{2cc}, taking into account a spin dependence of the radial integrals.

Moreover, an external magnetic field, H_z, can lift the ultimate degeneracy, essentially for the ions with odd number of electrons, and permits the determination of the Zeeman factor g.

III – PARAMETRIZATION OF THE MAIN INTERACTIONS

It is not possible to calculate exactly the effect of these interactions, only their order of magnitude can be estima-

ted. It is better to use a parametric method, where a reduced number of phenomenological parameters, numerical coefficients of the application of the tensorial operator equivalent to the interaction, permits to reproduce the spectrum. Table 2 shows the parameters involved. Naturally, the number of parameters depends on the configuration (for the free ion parameters and for the crystal field parameters (cfp), and on the symmetry of the ion site (for the cfp's). However, the phenomenological parameters don't vary freely, because Hartree-Fock calculations for the free ion parameters (table 3) or "ab-initio" models for the crystal field (table 4) give only their order of magnitude.

	Hartree Fock	Pr^{IV} free ion	$LaCl_3 : Pr^{3+}$
F_2	98723.	72550.	68368.
F_4	61937.	53681.	50008.
F_6	44564.	36072.	32743.
ξ	820.2	769.9	744.
α	28.	23.8	22.9
β	−615.	−613.2	−674.
γ	1611.	6745.7	1520.
M^0	1.99	1.59	1.76
P^2	–	–	275.

Table 3. Comparison between calculated and experimental rare earth free ion parameters (from W.T. Carnall, NATO Summer School, Braunlage, Germany 1982). Units in cm^{-1}

III.1 – Electrostatic repulsion

The matrix elements are written in a relatively simple way only for two equivalent electrons:

$$<(n\ell)^2\, SL|\, H_{RE}\, |(n\ell)^2\, SL> = \sum_k f_k(\ell,\ell)\, F^k(n\ell,n\ell)$$

where F^k are the Slater integrals and

$$f_k(\ell,\ell) = (-1)^L <\ell\, ||C^{(k)}||\, \ell>^2 \begin{Bmatrix} \ell & \ell & k \\ \ell & \ell & L \end{Bmatrix}$$

$\{\ \}$ is a 6j-symbol. For other configurations the matrix elements are deduced from these elements by a recursion method involving the fractional parentage coefficients.[4] An alternative way is to consider the Racah free ion parameters E_k, linear combination of the F_k's.

III.2 – The crystal field

In the Wybourne's formalism[4], the crystal field potential is written as a sum of products of tensorial operators:

$$H_{cf} = \sum_{k,q,i} B_{kq}\, (C_{kq})_i$$

In which C is the tensorial operator, having the same symetry rules as the spherical harmonics and B the phenomenological cfp's. The sum runs over all electrons of the system.

For a D_{4h} symmetry the potential is:

$$H_{4h} = B_{20} C_{20} + B_{40}\, C_{40} + B_{44}\, (C_{44} + C_{4-4})$$

When the symmetry is lowered to C_{2v}, two more cfp's are involved:

$$H_{2v} = H_{4h} + B_{22}\, (C_{22} + C_{2-2}) + B_{42}\, (C_{42} + C_{4-2})$$

On the $|\alpha SLJM>$ basis the matrix elements are written according to the Racah algebra rules:

$$<\alpha SLJM\, |\, H_{cf}\, |\alpha' S'L'J'M'> = \Sigma\, B_{kq}\, .\, \delta\,(SS')\, .$$

$$.\, <\alpha SLJM\, |\, U_q^{(k)}\, |\alpha' SL'J'M'><\ell\, ||C^{(k)}||\, \ell>$$

where

$$<\ell\, ||C^{(k)}||\, \ell> = (-1)^{\ell}(2\ell+1)\, \begin{Bmatrix} \ell & k & \ell \\ 0 & 0 & 0 \end{Bmatrix}$$

and

$$<\alpha SLJM\, |\, U_q^{(k)}\, |\alpha' S'L'J'M'> = (-1)^{J-M}$$

$$\begin{pmatrix} J & k & J' \\ -M & q & M' \end{pmatrix} (-1)^{S+L'+J+k} [(2J+1)\,(2J'+1)]^{1/2} \times$$

$$\times \begin{Bmatrix} J & J' & k \\ L' & L & S \end{Bmatrix} <\alpha SL\, ||U^{(k)}||\, \alpha' SL'>$$

In these expressions, the $<||C^{(k)}||>$ are the one electron reduced matrix elements ($\ell = 2$ for d configuration),

		B_{20}	B_{40}	B_{44}	B_{60}	B_{64}
$LiYF_4 : Nd^{3+}$	calc.	311.	−821.	1396	−10.	871.
	exp.	401.	−1008.	1230	30.	1074.
$KY_3F_{10} : Eu^{3+}$	calc.	−953.	−1396.	557.	829.	296.
	exp.	−528.	−1358.	368.	476.	−41.
$BaFCl : Sm^{2+}$	calc.	11.	−112.	−37.	429.	226.
	exp.	−92.	−163.	67.	394.	200.

Table 4. "Ab-initio" calculated and experimental crystal field parameters of rare earths in a quaternary symmetry case. (from D. GARCIA and M. FAUCHERI)[2].

( ) are 3j-symbols and $< ||U^{(k)}|| >$ are doubly reduced matriz elements as tabulated by Nielson and Koster[5].

One 3-j non-vanishing rule implies that $-M+q+M'=0$. With respect to the symetry point group, this creates subspaces to which the group irreducible representations are associated. When the spin orbit coupling is omitted, the crystal field potential can be translated on the $|SM_sLM_L>$ basis through the Clebsch-Gordan coefficients, and the B_{kq} easily related to D_q, D_s and D_t. The order of magnitude of the cfp's is 15000 cm^{-1} for 3d ions, to be compared with 1000 cm^{-1} for the 4f's (table 5).

III.3 – The spin-orbit coupling

On the $|\alpha SLJM>$ basis, the spin-orbit coupling lifts the term degeneracy. The matrix element is written as

$$<\alpha SLJM\,|\,H_{so}\,|\alpha'S'L'J'M'> = \xi\,\delta(JJ')\,\delta(MM')\,(-1)^{J+L+S'}\,[\ell(\ell+1)(2\ell+1)]^{1/2} \times \begin{Bmatrix} L & L' & 1 \\ S' & S & J \end{Bmatrix} <$$

$$<\alpha SL\,||\,V^{(11)}\,||\,\alpha'S'L'>$$

where ξ is the phenomenological parameter, $\ell = 2$ for d elements, and $V^{(11)}$ is a double tensorial operator. The reduced matrix elements are also found in the Nielson and Koster tables.[5] The ^{2S+1}L label of the term becomes $^{2S+1}L_J$ for the free ion level, the sub-spaces are not affected. The order of magnitude of the spin-orbit parameter is the same for 3d and 4f ions (table 5).

The full matrix we have to diagonalize is the sum of all contributions:

$$<\alpha SLJM\,|\,H\,|\alpha'S'L'J'M'> = <\alpha SLJM\,|\,H_E\,|\alpha'S'L'J'M'> + <\alpha SLJM\,|\,H_{cf}\,|\alpha'S'L'J'M'> + <\alpha SLJM\,|\,H_{so}\,|\alpha'S'L'J'M'> + \ldots.$$

After the diagonalization, the wavefunction is described on the entire sub-space basis: $|\Phi> = \sum_i a_i |\alpha SLJM>_i$

config.	F_2	ξ	$B_{k\,q}$
$3d^N$	70000.	500.	15000.
$4d^N$	50000.	1000.	20000.
$5d^N$	20000.	2000.	25000.
$4f^N$	70000.	1500.	1000.
$5f^N$	50000.	2500.	2000.

Table 5. Order of magnitide of the main parameters. Units in cm^{-1}.

IV – PARAMAGNETIC SUSCEPTIBILITY AND EFECTIVE MOMENT

The paramagnetic susceptibility is calculated by the Van Vleck formula:

$$\chi = N\beta^2 \sum_a \frac{<\Phi_a|H|\Phi_a>^2}{KT} - 2\sum_b \frac{<\Phi_a|H|\Phi_b><\Phi_b|H|\Phi_a>}{E_a - E_b}\,.B_a$$

in which N is the Avogadro number, β the Bohr magneton, K the Boltzman constant, E and Φ the non perturbated eigenvalues and wavefunctions, respectively. Here H is the magnetic tensorial operator $L+g_eS$. The sum runs over thermally populated levels, according to Boltzman's population B_a. In this expression, the matrix elements are calculated by using the Racah algebra rules. The effective moment μ_{eff} is related to χ by $\mu_{eff} = 2.828\sqrt{\chi T}$. The calculation is performed as a perturbation. Of course it is always possible to introduce the operator H in the secular determinant before diagonalisation (breaking the remaining degeneracies of Kramers doublets), but this is not necessary due to the smallness of the perturbation.

The expression is the sum of a temperature-dependent diagonal term, and a temperature-independent off-diagonal term, which reminds the classical Curie-Weiss law. The off-diagonal term results from the second order perturbation and has usually a small importance with the exception of ground states with $J=0$. The sum runs over all other states ($b \neq a$). Rare earths show that the calculation is in good agreement with experiment.[6] The best proof is obtained from the Europium ion case with $^7F_0$ as ground state; the value of the plateau, depending only on the off-diagonal term, is well reproduced[7] (fig. 1).

For d elements we consider the paramagnetic susceptibility as a part of the simulation, completing the energy level sequence. There are two possibilities:

1) to carry out a computational minimization between calculated and experimental χ (or μ_{eff}). The steps are the followings: first a diagonalization of the secular determinant with a starting set of parameters, next the derivation of the obtained wavefunctions with respect to phenomenological parameters, the minimization of the equation yielding new parameters for a new diagonalization, and so on... This procedure is rather heavy and not safe, since the minimization procedure is not linear.
2) from approximate values of parameters (fitting roughly the energy level scheme) we can operate by graphics. This procedure was adopted.

Let us consider the case of the Co^{2+} ion (d^7 configuration). By varying B_{2o} and B_{4o} in their possible values, we obtain a map, one for each temperature (4, 77 and 300K

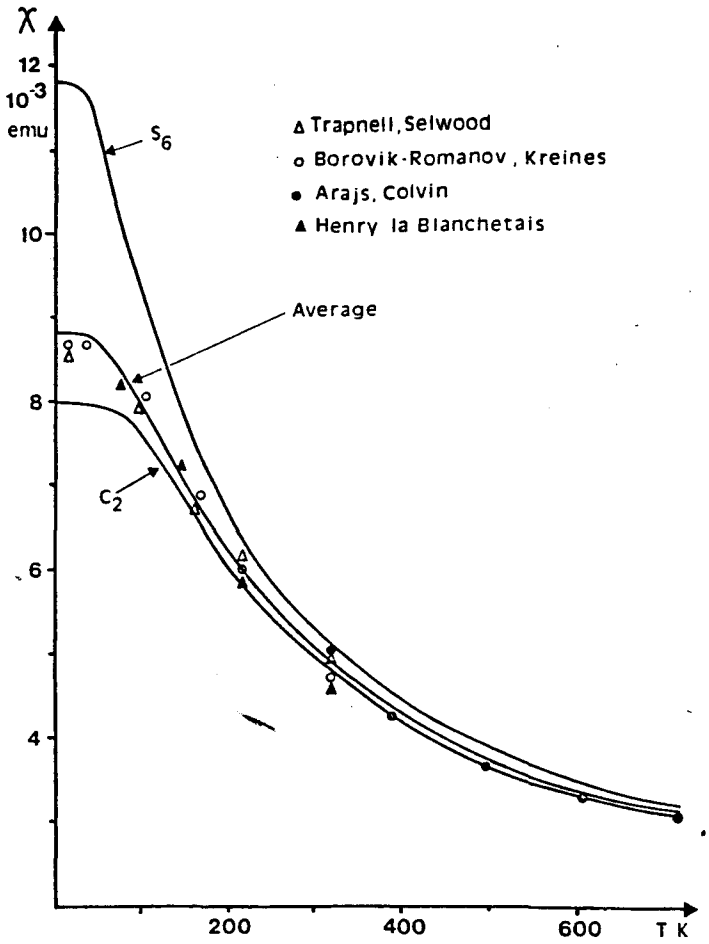

Figure 1. Paramagnetic susceptibility of Eu_2O_3 (C-type). The structure comprises two point sites of different symmetry. For each, the cfp set is derived from the optical data. Each site gives its own contribution to the paramagnetic susceptibility. The sum corresponds to the experiment (from Caro & Porcher 1986)[7]

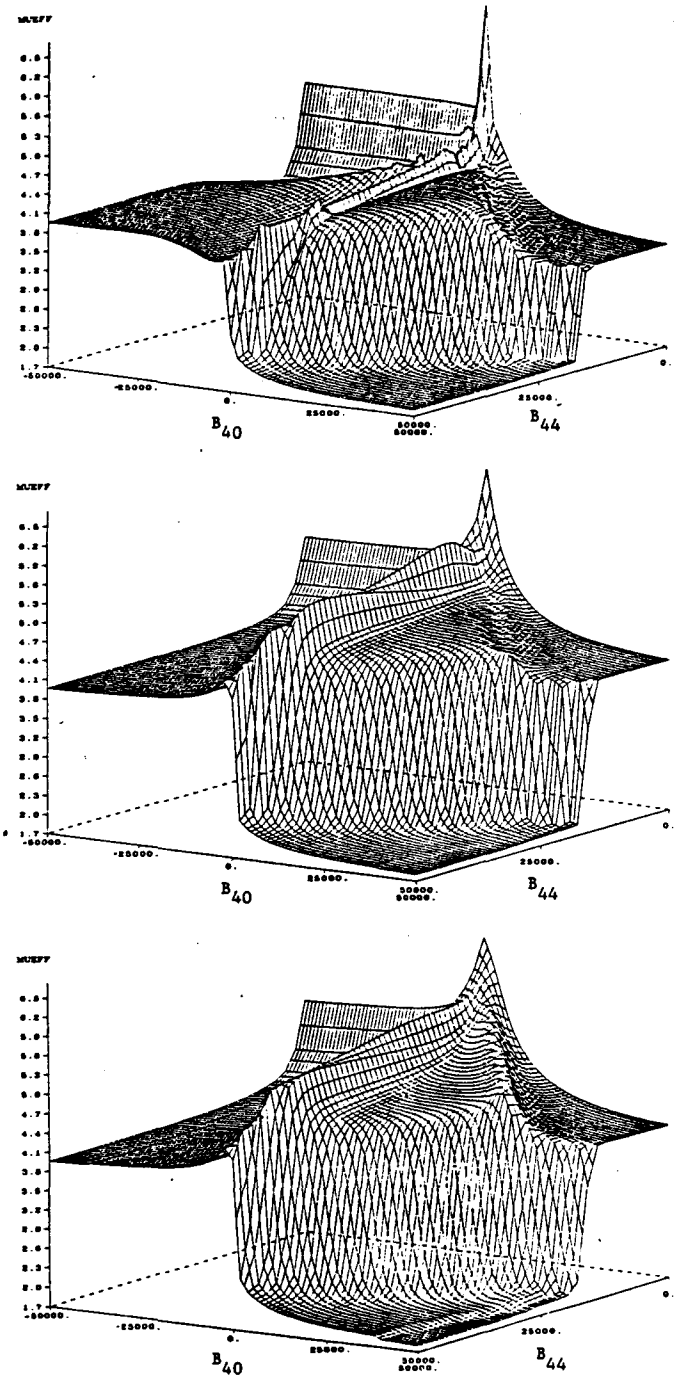

Figure 2. Effective moment μ_{eff} of Co^{2+} (d^7 configuration) $B_{2\,0} = 0$. cm^{-1} and $\xi = 500\ cm^{-1}$

in fig. 2). The map shows valleys, plateaux, cliffs and pics. At first order, the effective moment varies with temperature essentially by creation of valleys and modifying the abruptness of the slopes. The high-spin → low-spin transitions are clearly distinguished.

V – CALCULATION OF g

The g calculation is quite similar to that of the paramagnetic susceptibility. The same $L+g_eS$ tensorial operator is applied on the wavefunction of a level. The g value is non vanishing only for Kramers doublets. The three components of g have the form:

$$g = \{<\Phi^+|L+g_eS|\Phi^+>^2 + <\Phi^+|L+g_eS|\Phi^->^2\}^{1/2}$$

In that expression, the two parts of the sum correspond to the application of the wavefunction on itself $<+, +>$ and on its Kramers conjugated $<+, ->$. The sign is arbitrarily decided as the one of $<+, +>$ matrix element for $g_{//}$ and of $<+, ->$ for $g_\perp$. Of course, the sign is not derived from EPR measurements, but can be checked from MCD[8]. When the symetry is at least binary, the non-zero rules for 3j-symbols give:

$$g_{//} = <\Phi^+|(L+g_eS)_0|\Phi^+>$$

$$g_\perp = <\Phi^+|(L+g_eS)_{\pm 1}|\Phi^->$$

g_x and g_y are normalised combinations of the tensor com-

ponents ±1. By varying the cfp's, we can construct a series of graphs corresponding to the g's of the ground level, whose values are the most often cited in the literature. The topology of the system is simpler: only plateaux and falls. Fig. 3 shows a series of graphs with various B_{44} for the case of a quaternary symmetry of the Cu^{2+} ion (d^9). B_{20} and B_{40} vary within their probable values. Three plateaux appear, well separated, corresponding to the different cases of irreducible representations for the ground level. Naturally, the most interesting is the transition zones, where situations are not clearly defined, with g values far from those determined by applying the first order perturbation theory. One transition zone of $g_{//}$, corresponding to an abrupt fall and to a pit on the curves, is not clearly understood, occurring when $^2E_7$ and ^2B irreducible representations of the ground level cross. The position of the plateaux, in terms of g values, is very dependent on B_{44} (D_q), allowing the determination of its value. The plateaux are not exactly horizontal, having a very small slope. For example, a variation of 0,001 for $g_{\perp}$ (usual precision of the measurement) corresponds to a variation of 300 cm^{-1} for the doublet energy and about 500 cm^{-1} for one of the linear cfp's. This underlines the sensitivity of the method.

VI – AN EXAMPLE OF SIMULTANEOUS SIMULATION OF OPTICAL AND MAGNETO-OPTICAL DATA: DIVALENT COPPER IN TETRAGONAL OR PSEUDO -TETRAGONAL SYMMETRIES

The optical and magneto-optical properties of divalent copper embedded in complexes have been extensively studied since forty years. In a recent paper[9], we considered 20 compounds, 13 with D_{4h} point symmetry for the copper, 7 with a lower symmetry, treated as C_{2v}, slightly distorted from a quaternary symmetry. Two types of data are considered: optical and g values. From absorption, 2, sometimes 3, transitions are recorded. As usual, the lines are wide and some positions are deduced by deconvolution of broad bands. Some papers give data both at liquid nitrogen and at room temperature. From EPR, two (for D_{4h} symmetries) or three (for C_{2v} symmetries) values of g are measured. Moreover some rare magnetic susceptibility results are mentioned in the literature, i.e., some values for the effective moment at room temperature.

We consider 4 parameters (6 for C_{2v}): 3 (resp. 5) cfp's and the spin-orbit parameter. They have not the same effect and their values strongly affect the composition of the wavefunctions.

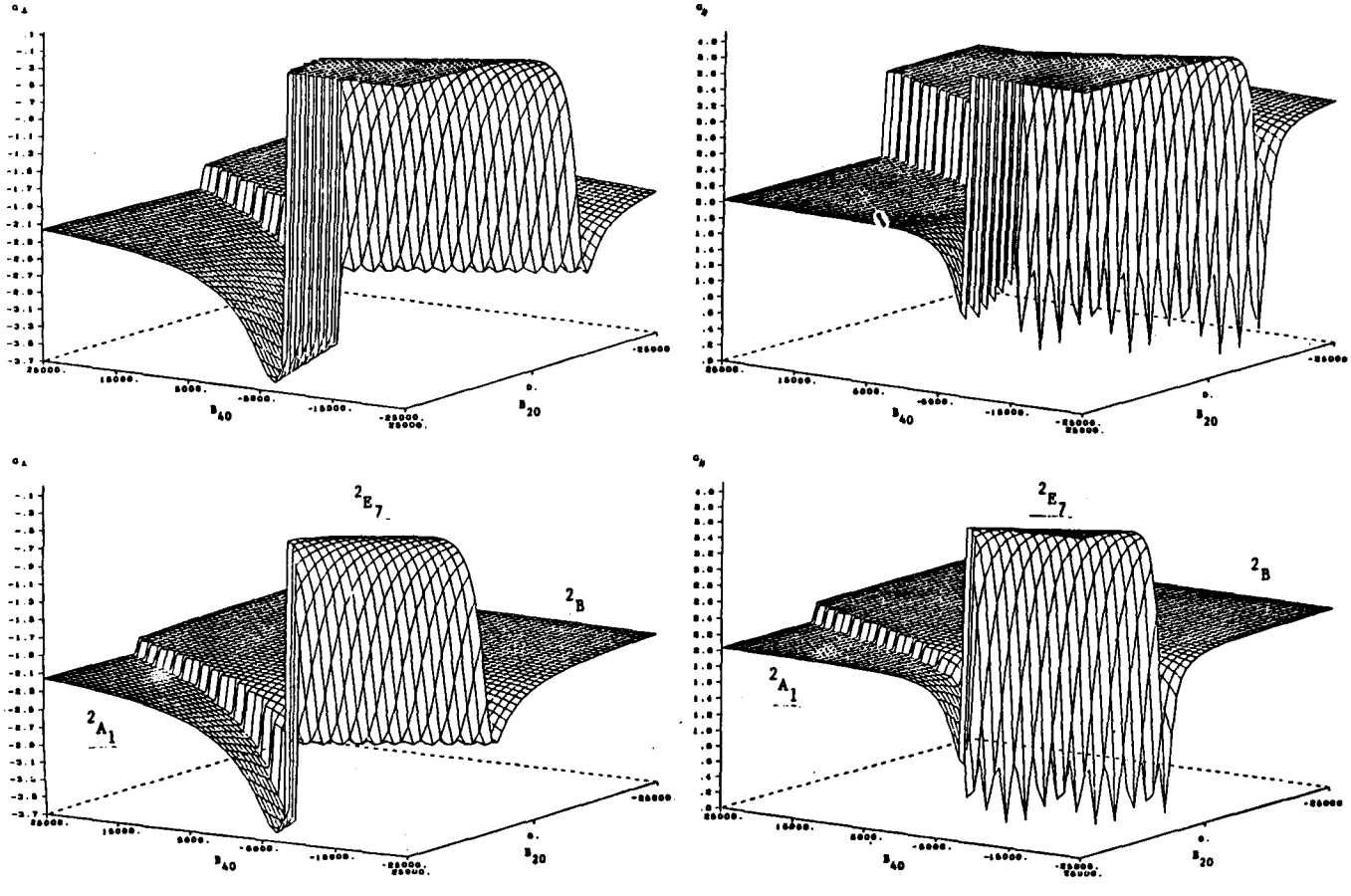

Figure 3. g values of Cu^{2+} (d^9 configuration) for different $B_{4\,4}$ values. 5000. cm^{-1} (top) and 25000. cm^{-} (bottom). The spin-orbit coupling constant is set to 500. cm^{-1}.

Under a quaternary symmetry, the d^9 configuration is split into two sub-spaces of Kramers doublets Γ_6 and Γ_7, even when spin-orbit interactions are considered. The solution of the secular determinant is equivalent to diagonalize two independant matrices whose dimensions are 3 for Γ_7 and 2 for Γ_6. The levels are easily related to the classical d orbitals (when without spin-orbit) and the ket's composition defined. The effect of the spin-orbit interaction is to split the doublet by some hundreds cm^{-1}. The positions of others levels are affected. Two transitions become possible: $B_1 \rightarrow E_6$ and $B_1 \rightarrow E_7$.

From this series of simulations, interesting features appear. The value of B_{44} does not vary too much. This parameter, directly proportional to D_q, is very dependent on the planar ligands. On the contrary, the linear parameters B_{ko}, vary more significantly along the series. They are more the result of the axial ligand contribution. Moreover, when low and room temperature spectra are known, they vary much more (up to 30%) than B_{44} (up to 3%). The variation of the cfp's due to the thermal contraction of the network, is a well known phenomenon for the rare earths. For the d electrons, the absolute magnitude of the cfp's is larger and this temperature dependance can be one reason for the high-spin → low-spin transitions and their consequences on the magnetic properties.[10] In all cases cfp's values are far from the cubic ratio. Only by looking at the large value of B_{20}, it is evident that the procedure which considers a cubic potential, and applies after a perturbative potential, is not precise enough. The starting symmetry of the simulation has to be considered as near as possible to the real point site symmetry.

The spin-orbit coupling constant varies significantly from one compound to another. Not only, the spin-orbit effect has to be taken into account in the simulation (and we mean not like a perturbation), but its average value (530 cm^{-1}) is lowered with respect to the calculated free ion one (830 cm^{-1}). The same occurs for the rare earths, but not so much (typically 15%). It is noteworthy that the ratio between experimental and calculated values corresponds more or less to the usual reduction factor[3], but without anisotropy. The parameter ξ varies relatively more around its average value (± 15%) than for the rare earths (± 3%). This variation can be understood in terms of the nephelauxetic effect, i.e., bonding effects.[11] The same is also observed for the Slater integrals, F_k, more particularly for F_2 (when they appear).

ACKNOWLEDGEMENTS

One of us (O.L.M.) is grateful to the CNPq for financial support.

REFERENCES

[1] Gschneider, K.A.Jr.; Eyring, L. (Eds.); *"Handbook on the Physics and Chemistry of Rare Earths"*; North-Holland.
[2] Garcia, D.; Faucher, M.; *J.Chem.Phys.* (1985) *82,* 5554.
[3] Stevens, K.W.H.; *Revs.Mod.Phys.* (1953) *A25,* 166.
[4] Wybourne, B.G.; *"Spectroscopic Properties of Ions in Crystals"*; Interscience, N.York (1965).
[5] Nielson, C.W.; Koster, G.F.; *"Spectroscopic Coefficients for p^N, d^N and f^N configurations"*; MIT Press (1964).
[6] Antic - Fidancev, E.; Lemaitre – Blaise, M.; Beaury, L.; Teste de Sagey, G.; Caro, P.; *J.Chem.Phys.* (1980) *73,* 4613.
[7] Caro, P.; Porcher, P.; *J.Mag.Magn.Mat.* (1986) *58,* 61.
[8] Gorller-Walrand, C.; Behets, M.; Porcher, P.; Laursen, I.; *J.Chem.Phys.* (1985) *83,* 4329.
[9] Bailleul, S.; Porcher, P.; to be published.
[10] Caro, P.; Derouet, J., Porcher, P.; *C.R. Acad. Sci. Paris* (1985) 301 II, 910.
[11] Antic-Fidancev, E.; Lemaitre-Blaise, M.; Caro, P.; *New J. of Chem.* (1987) *11,* 469.